ORIGINAL RESEARCH ARTICLE

Drug Safety 2009; 32 (7): 599-611
0114-5916/09/0007-0599/$49.95/0

Identifying Drug-Induced Repolarization Abnormalities from Distinct ECG Patterns in Congenital Long QT Syndrome

A Study of Sotalol Effects on T-Wave Morphology

Claus Graff,[1] *Mads P. Andersen*,[1] *Joel Q. Xue*,[2] *Thomas B. Hardahl*,[1] *Jørgen K. Kanters*,[3,4,5] *Egon Toft*,[1,5] *Michael Christiansen*,[6] *Henrik K. Jensen*[7] and *Johannes J. Struijk*[1]

1 Centre for Sensory Motor Interaction (SMI), Department of Health Science and Technology, Aalborg University, Aalborg, Denmark
2 GE Healthcare, Milwaukee, Wisconsin, USA
3 Department of Cardiology P, Gentofte University Hospital, Gentofte, Denmark
4 Danish National Research Foundation, Centre for Cardiac Arrhythmia (DARC), University of Copenhagen, Copenhagen, Denmark
5 Department of Cardiology S, Aalborg Hospital, Aarhus University Hospitals, Aalborg, Denmark
6 Statens Serum Institute, Copenhagen, Denmark
7 Department of Cardiology B, Aarhus University Hospital Skejby, Aarhus, Denmark

Abstract

Background: The electrocardiographic QT interval is used to identify drugs with potential harmful effects on cardiac repolarization in drug trials, but the variability of the measurement can mask drug-induced ECG changes. The use of complementary electrocardiographic indices of abnormal repolarization is therefore warranted. Most drugs associated with risk are inhibitors of the rapidly activating delayed rectifier potassium current (I_{Kr}). This current is also inhibited in the congenital type 2 form of the long QT syndrome (LQT2). It is therefore possible that electrocardiographic LQT2 patterns might be used to identify abnormal repolarization patterns induced by drugs.

Objective: To develop distinct T-wave morphology parameters typical of LQT2 and investigate their use as a composite measure for identification of d,l-sotalol (sotalol)-induced changes in T-wave morphology.

Methods: Three independent study groups were included: a group of 917 healthy subjects and a group of 30 LQT2 carriers were used for the development of T-wave morphology measures. The computerized measure for T-wave morphology (morphology combination score, MCS) was based on asymmetry, flatness and notching, which are typical ECG patterns in LQT2. Blinded to labels, the new morphology measures were tested in a third group of 39 healthy subjects receiving sotalol. Over 3 days the sotalol group received 0, 160 and 320 mg doses, respectively, and a 12-lead Holter ECG was recorded for 22.5 hours each day. Drug-induced prolongation of the heart

rate corrected QT interval (QTcF) was compared with changes in the computerized measure for T-wave morphology. Effect sizes for QTcF and MCS were calculated at the time of maximum plasma concentrations and for maximum change from baseline. Accuracy for separating baseline from sotalol recordings was evaluated by area under the receiver operating characteristic curves (AUCs) using all recordings from the time immediately postdose to maximum change.

Results: MCS separated baseline recordings from sotalol treatment with higher accuracy than QTcF for the 160 mg dose: (AUC) 84% versus 72% and for the 320 mg dose: (AUC) 94% versus 87%, $p < 0.001$. At maximum serum-plasma concentrations and at maximum individual change from baseline, the effect sizes for QTcF were less than half the effect sizes for MCS, $p < 0.001$. Effect sizes at peak changes of the mean were up to 3-fold higher for MCS compared with QTcF, $p < 0.001$. In subjects receiving sotalol, T-wave morphology reached similarity to LQT2, whereas QTcF did not.

Conclusion: Distinct ECG patterns in LQT2 carriers effectively quantified repolarization changes induced by sotalol. Further studies are needed to validate whether this measure has general validity for the identification of drug-induced disturbed repolarization.

Background

The vast majority of drugs exert their QT prolonging effect through inhibition of the rapidly activating delayed rectifier potassium current (I_{Kr}),[1] which is encoded by *KCNH2* (the human ether-à-go-go-related gene, hERG).[2] I_{Kr} channel blockade is one of the most common causes of drug withdrawal from the market[3,4] because blockade of this channel has been associated with torsades de pointes (TdP), ventricular tachycardia and sudden cardiac death. hERG mutations are known to provide the pathogenic substrate for I_{Kr} channel inhibition in congenital type 2 form of the long QT syndrome (LQT2)[5] and a direct link between inherited and drug-induced long QT syndrome has been established.[6] On the ECG, I_{Kr} channel inhibition manifests as a prolonged QT interval[7] and the emergence of characteristic T-wave abnormalities.[8,9] Specifically, the presence of notches,[10-12] asymmetry[13-15] and the appearance of flat T-waves[16-18] have been found to be consistent with the ionic mechanism of I_{Kr} blockade. Abnormally shaped T-waves frequently appear without overt QT prolongation[19] and important abnormalities of the repolarization sequence may not be identified by the QT interval, which characterizes only the total duration of depolarization and repolarization.

Various parameters have been suggested as alternatives to QT interval measurements. QT dispersion is perhaps the best known and most widely investigated parameter, but it has not been successful in predicting drug-induced risk.[20] Experimental evidence from the wedge model has suggested that the Tpeak-Tend interval (TpTe) reflects heterogeneity of repolarization.[21] In the wedge model, it was shown that d,l-sotalol (sotalol) increased dispersion across the ventricular wall and that such I_{Kr} blocking conditions were accompanied by prolongation of TpTe and QTc, a reduced T-wave amplitude and the appearance of LQT2-like notches.[21] In a recent study, the duration of TpTe was found to correlate with increased risk for TdP during acquired bradyarrhythmias in humans, particularly in the presence of LQT2-like notched T-waves.[22]

T-wave alternans has been reported with congenital long QT syndrome[23] and appears to be an important indicator in that it is commonly observed just prior to episodes of TdP. Recently, the beat-to-beat variability of repolarization duration was shown to determine drug-induced proarrhythmic outcome in the dog.[24] In the clinical setting, beat-to-beat variability distinguished between patients with documented history of drug-induced TdP and absence of QT prolongation from their matched controls,[25] and the measurement was a predictor of sudden cardiac death in patients with myocardial infarction.[26] These results suggest that beat-to-beat variability of the QT interval might be used to identify patients at risk by unmasking a latent repolarization disorder. The repolarization integral has been shown to discriminate between KvLQT1 and hERG mutations in the congenital long QT syndrome[9] and a set of T-wave area-based measures in subjects receiving sotalol indicated that drug-induced shape changes occur across the entire repolarization segment.[27]

Accumulating evidence thus suggests that a number of ECG markers of repolarization hold the potential to complement the QT interval for cardiac safety evaluation. The possible integration of ECG markers into a composite descriptor of T-wave shape characteristics might provide a new opportunity to describe and understand repolarization abnormalities in the congenital and acquired forms of the long QT syndrome. A validated quantitative descriptor of composite T-wave morphology is currently lacking, although the morphology of the T-wave could be of greater importance than the QT interval for the assessment of proarrhythmic risk. In regulatory guidance notes for drug trials, an integrated risk assessment is mandatory.[28] This includes a full description of all ECG changes, including T-wave morphology.

The present study investigates ECG manifestations of repolarization abnormalities induced by the torsadogenic drug sotalol to determine whether a composite ECG measure based on typical LQT2 patterns of T-wave morphology can provide an effective description of the sotalol-induced ECG changes.

Methods

Study Design

Three different study groups were compared in the study. A first group of healthy volunteers (group 1) served as an electrocardiographic reference for normal repolarization, and a second group of LQT2 carriers (group 2) served as an electrocardiographic reference for abnormal repolarization. A third group of subjects receiving sotalol (group 3) were compared with group 1 before sotalol was given, and compared with group 2 after sotalol was given. Intra-individual changes from baseline (individual and mean) were calculated for the sotalol group at the time of maximum plasma concentrations and for maximum change from baseline. Effect sizes were calculated to determine the magnitude of change from baseline for the sotalol group. The area under receiver operating characteristic (ROC) curves (AUC) was used to determine test accuracy as the ability of heart rate corrected QT interval (QTcF) and T-wave morphology to distinguish between all baseline and treatment recordings (dichotomized to 0 and 1, respectively) from the time immediately post-dose to maximum treatment effects. Sensitivities and specificities for QTcF and T-wave morphology measures were derived from ROC curves.

Study Population

There were 917 healthy individuals (771 men, 146 women; age 18–45 years; mean ± standard deviation [SD] = 29 ± 7 years) in group 1. The inclusion/exclusion criteria for group 1 subjects were comparable with the criteria generally used in ECG phase I investigations, with healthy status confirmed by history, physical examination, normal blood pressure and no use of medications.

The LQT2 group (group 2) included 30 genetically confirmed hERG mutation carriers (19 women, 11 men; age 19–68 years; mean ± SD = 45 ± 14 years). There were nine families with eight different mutations. At the time of ECG recordings, 24 LQT2 patients were taking a β-adrenergic receptor antagonist. There were

19 symptomatic LQT2 patients. All subjects gave informed consent.

An independent third group of 39 healthy subjects (11 women, 28 men; age 18–45 years; mean ± SD = 27 ± 8 years) were given sotalol (group 3). The sotalol data were obtained during 3 consecutive days at Pharmacia's Clinical Research Unit (Kalamazoo, MI, USA). The details of the protocol have previously been published.[29] No drug was provided during the first 24 hours (day 1), a single 160 mg dose of sotalol (Betapace® 80 mg tablets, Berlex Laboratories Montville, NY, USA) the following day (day 2) and a single 320 mg dose of sotalol on the final day (day 3). Blood plasma concentration was measured 16 times on days 2 and 3. A baseline Holter was recorded on day 1. All 39 subjects received a 160 mg dose of sotalol on day 2, and 22 of them (all males) also received a 320 mg dose on day 3. Seventeen subjects were withdrawn after the 160 mg dose as previously described[29] and one subject was excluded from analysis due to poor Holter ECGs on the final study day. An independent Institutional Review Board approved the sotalol study.

ECG Acquisition

From each healthy subject (group 1) and each LQT2 subject (group 2), a standard 12-lead digital ECG of 10 seconds duration was recorded at a sample rate of 500 Hz (MAC5000, GE Medical Systems, Milwaukee, WI, USA). Data from group 1 were acquired from the GE-Marquette research database of healthy volunteers. Data from group 2 were recorded at Aalborg University Hospital (Aalborg, Denmark), the Long QT Syndrome Clinic in Gentofte University Hospital (Gentofte, Denmark) and Skejby University Hospital (Aarhus, Denmark). Collection of clinical data for LQT2 patients was approved by the Scientific Ethical Committee for Nordjylland and Viborg (no.: vn/2003/129).

ECG data from the sotalol group (group 3) were recorded at Pharmacia's Clinical Research Unit (Kalamazoo, MI, USA) with 12-lead digital Holter at a sample rate of 180 Hz (H12 Recorder, Mortara Instrument, Milwaukee, WI, USA). Each 10-second ECG extracted from Holter was resampled to 500 Hz. From each subject, 22.5-hour recordings were obtained per day. At approximately 30-minute intervals, 12-lead ECGs of 10 seconds duration were derived from Holter. To ensure stability of repolarization, a representative 10-second segment was extracted from Holter, only if it was preceded by 1 minute of visually stable heart rate. Care was taken to select the most visually noise-free segments with stable RR intervals (the time elapsing between two consecutive R waves on the ECG) and all representative median beats were derived from such stable and noise-free 10-second Holter segments.

ECG Preprocessing

Each 10-second ECG was used to form a median beat in the recorded leads using MUSE/Interval Editor software (GE Healthcare, Milwaukee, WI, USA). It has been shown that morphological description of the T-wave in long QT syndrome should not be restricted to any single lead.[30] In line with those recommendations, global leads were formed from principal component decomposition of the median beats by principal component analysis. A low-pass Kaiser Window FIR filter with a cutoff frequency of 20 Hz was used on the first global lead (first principal component ECG). The filtered T-wave from the first global lead was subsequently used for analysis of repolarization morphology. Fiducial point detection and QT measurements were made automatically using the 12SL algorithm (12SL, GE Healthcare, Milwaukee, WI, USA). The algorithm excludes discrete U waves that occurred after the T-wave return to baseline from analysis, whereas complex, multiphasic T-waves and T-U complexes are included. QT intervals were corrected for heart rate with Fridericia's equation: $QTcF = QT/RR^{1/3}$. The morphology measures that were investigated in the present study were not corrected for heart rate because it was recently shown that they are practically independent of heart rate.[31]

Morphology Measures

A morphology combination score (MCS) was developed to describe differences in T-wave

asymmetry, flatness and notching between the two open-label datasets consisting of 917 healthy subjects as representatives of normal repolarization (group 1) and 30 LQT2 subjects as a biological model of I_{Kr} channel inhibition (group 2). Subsequently, the MCS measure was used as a test in the sotalol group (group 3) blinded to the analyst. Labels for the sotalol subjects were disclosed after the MCS results were released from the ECG analyst.

The variables comprising MCS were standardized by their relative variances for LQT2 and healthy subjects (equation 1).

$$MCS = Asymmetry + Notch + 1.6 \times Flatness \quad \text{(Eq. 1)}$$

This standardization effectively gives each variable equal importance in the composite score. Equal weighting is appealing when a change in each variable does not mean redundancy of information in the composite score, i.e. when the component variables explain different aspects of abnormal repolarization that the composite measure should capture.

Asymmetry

The difference in slopes of the ascending and descending parts of the T-wave was considered a measure of asymmetry. The slopes at each point of the descending part of the T-wave were mirrored to be compared with the slopes at corresponding points of the ascending segment. Asymmetry was defined as the average squared difference between the slope segments.[32]

Notch

A curvature signal, which measures how fast a curve is changing direction at a given point, was obtained from the first and second derivatives of T-waves. This signal indicates the presence of notches because deflections in curvature correspond to deviations from the normal smooth progress of a T-wave. The magnitude of a notch was measured on a unit amplitude T-wave and assigned to one of three categories as previously suggested:[12] no deflection = 0, moderate notch (perceptible bulge) = 0.5 and pronounced notch (distinct protuberance above the apex) = 1.0.

Flatness

T-wave amplitudes were normalized to yield a unit area under the T-wave curve. From this signal, flatness was calculated using instantaneous amplitudes, the weighted mean and the variance, analogous to the way kurtosis is calculated from a sample distribution.[32]

Statistical Analysis

All statistical analyses were performed in SPSS 12.0 for Windows (SPSS Inc., Chicago, IL, USA). Intra-subject differences were evaluated by paired Student's t-tests for the sotalol group. Unpaired t-tests were applied for two-sample observations involving healthy subjects (group 1) and LQT2 patients (group 2). Two-sided p-values were determined in all cases and $p < 0.05$ was regarded as significant. Glass' effect size measure of the z-score[33] was determined for the sotalol group to quantify the change from baseline in terms of standard deviations (equation 2). Glass' Δ was used to estimate effect size because equal variances could not be assumed before and after drug administration.

$$\text{Effect size} = \frac{\text{mean (drug} - \text{baseline)}}{\text{standard deviation (baseline)}} \quad \text{(Eq. 2)}$$

Importantly, because effect sizes are standardized they allow ready comparison of the magnitude of change with clinical trial benchmarks such as the QT interval. ROC sensitivities and specificities were determined from the point of inflection on ROC curves (nearest to top left corner). For AUC comparisons, the correlation between areas that is induced by the paired nature of the data was taken into account.[34]

Results

Baseline Means

There was no difference in the means for QTcF or T-wave morphology between healthy subjects and sotalol subjects prior to drug administration (table I). At the same time, the means for QTcF and T-wave morphology were significantly lower for sotalol subjects before the drug was given compared with the LQT2 group.

Table I. Comparison of mean values for patients with the type 2 form of the long QT syndrome (LQT2) and healthy subjects to mean values for sotalol subjects[a]

Study group	No.	QTcF (mean ± 1 SD) [ms]	MCS (mean ± 1 SD)
LQT2 patients	30	483 ± 35	1.80 ± 0.60
Healthy subjects	917	407 ± 18	0.71 ± 0.24
Sotalol (2.5 h)[b]			
no drug	39	408 ± 17*†	0.71 ± 0.19*†
no drug	21	403 ± 15*†	0.66 ± 0.11*†
160 mg	39	440 ± 36	1.24 ± 0.53
160 mg	21	426 ± 23	1.09 ± 0.37
320 mg	21	453 ± 21	1.72 ± 0.50‡
Sotalol (3.5 h)[b]			
no drug	39	404 ± 19*†	0.68 ± 0.12*†
no drug	21	400 ± 18*†	0.65 ± 0.11*†
160 mg	39	442 ± 24	1.40 ± 0.51
160 mg	21	435 ± 20	1.20 ± 0.34
320 mg	21	459 ± 14	1.82 ± 0.48§

a 2.5 h = maximum mean plasma concentration; 3.5 h = maximum change of the means for QTcF and MCS. All post-dose measures (2.5 and 3.5 h) for QTcF and MCS increased significantly from their time-matched pre-dose measures ($p < 0.001$).

b Two sets of subject data are presented. Where n = 39 the data are for all subjects, including those who did not receive sotalol 320 mg; where n = 21 the data are only for those subjects who received both doses of sotalol.

MCS = morphology combination score; **QTcF** = heart rate corrected QT interval; **SD** = standard deviation; * $p < 0.001$ vs LQT2; † not significant vs healthy subjects; ‡ $p = 0.62$ vs LQT2; § $p = 0.90$ vs LQT2.

Peak Changes of the Means

After sotalol was given, there were significant time-matched changes in the means for both T-wave morphology and QTcF (table I). Nine subjects of 21 developed notched T-waves when the 160 mg dose was given. For the 320 mg dose, this number increased to 19 subjects. There was a significant progression of T-wave flatness that reached a maximum change from baseline 3.5 hours post-dose for both the 160 and 320 mg doses (mean ± SD: [baseline] 0.54 ± 0.08 vs [160 mg] 0.80 ± 0.07 and [320 mg] 0.91 ± 0.07), $p < 0.001$ (figure 1). The degree of T-wave asymmetry increased after sotalol was given, with significant mean changes from baseline for 160 and 320 mg doses (mean ± SD: [baseline] 0.10 ± 0.06 vs [160 mg] 0.31 ± 0.13 and [320 mg] 0.57 ± 0.23), $p < 0.001$. For sotalol 320 mg, the peak value of mean QTcF (459 ms) remained below the mean QTcF for LQT2 (483 ms), $p = 0.004$, whereas T-wave morphology reached the level of LQT2 after the 320 mg dose (table I).

The number of standard deviations by which the mean MCS changed from baseline for the 160 mg dose was 2.7-fold greater than the corresponding QTcF change for 160 mg dose, 5.28 (95% CI 3.51, 7.05) versus 1.97 (95% CI 1.20, 2.74), $p < 0.001$ (figure 2). For the 320 mg dose, MCS changed by 11.10 standard deviations from baseline (95% CI 7.51, 14.69). This effect size was 3.3-fold larger than the observed effect size for QTcF, 3.32 (95% CI 2.15, 4.49), $p < 0.001$ (figure 2).

Test Accuracy

From the time immediately post-dose (0.5 hours) to the largest response in the mean (3.5 hours), T-wave morphology discriminated between baseline recordings and sotalol treatment with significantly higher accuracy compared with QTcF prolongation (table II). The use of equal weights in the MCS was justified by the observation that test accuracy did not improve with differential weighting (DW) of morphology indicators (MCS-DW) in a logistic regression model that was trained *post hoc* with baseline and 320 mg recordings: $MCS\text{-}DW = asymmetry + 2.4 \times notch + 2.1 \times flatness$. The AUCs were similar for MCS with equal weights and MCS-DW with differential weights for the 160 mg dose ($AUC_{MCS\text{-}DW}$ ± 1 SE, 83 ± 2%) and the 320 mg dose ($AUC_{MCS\text{-}DW}$ ± 1 SE, 94 ± 1%).

Furthermore, in a logistic regression model that was trained *post hoc* on the same sotalol data with inclusion of QTcF in the T-wave morphology measure (MCS-QT): $MCS\text{-}QT = asymmetry + 2.2 \times notch + 2.1 \times flatness + 0.001 \times QTcF$, an increase for MCS in the accuracy of separating baseline recordings from sotalol treatment could not be demonstrated (figure 3). The AUCs were similar for MCS and MCS-QT for both the 160 mg dose ($AUC_{MCS\text{-}QT}$ ± 1 SE, 82 ± 2%) and the 320 mg dose ($AUC_{MCS\text{-}QT}$ ± 1 SE, 94 ± 1%).

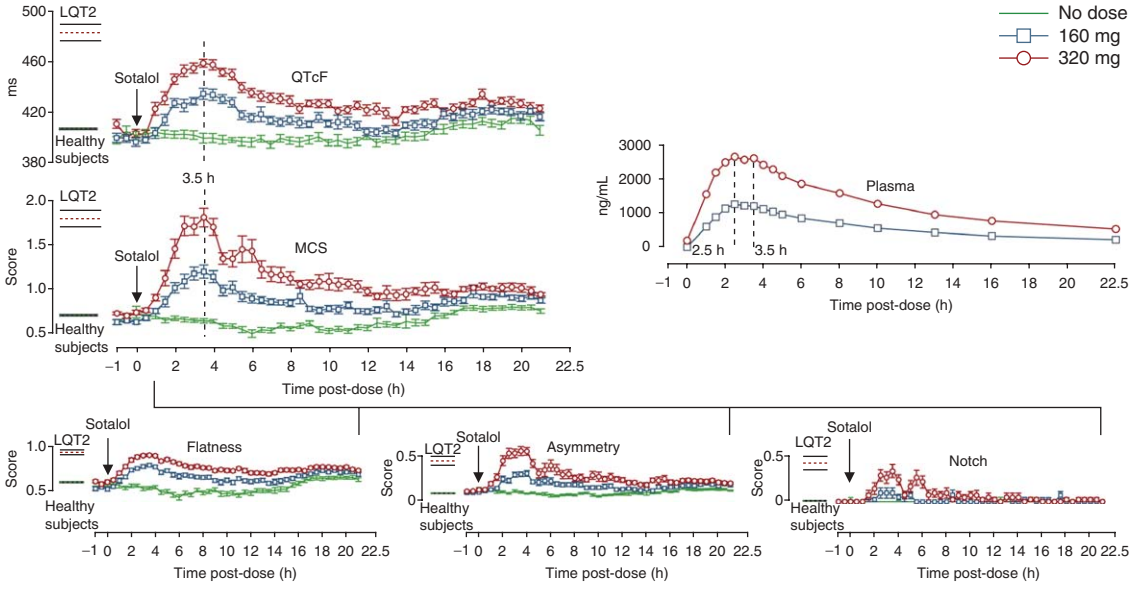

Fig. 1. Heart rate corrected QT interval (QTcF) and T-wave morphology in relation to plasma concentrations and time of sotalol administration. Horizontal dotted and solid black lines indicate the mean values of the healthy subjects (group 1) and patients with the type 2 form of the long QT syndrome (LQT2) [group 2] ±1 standard error (SE) of the mean. Curves show mean values of 21 subjects (group 3) before and after sotalol administration ±1 SE. **MCS** = morphology combination score.

Maximum Individual Changes

The average of individual maximum drug effects on T-wave morphology was significantly larger than the average of maximum effects on QTcF prolongation when changes were evaluated at the times of subject-specific peak plasma concentrations (C_{max}) and subject-specific maximum changes from baseline (Δ_{max}) [table III]. At C_{max} for the 160 mg dose, T-wave morphology changed from baseline by an average number of standard deviations that was similar to the

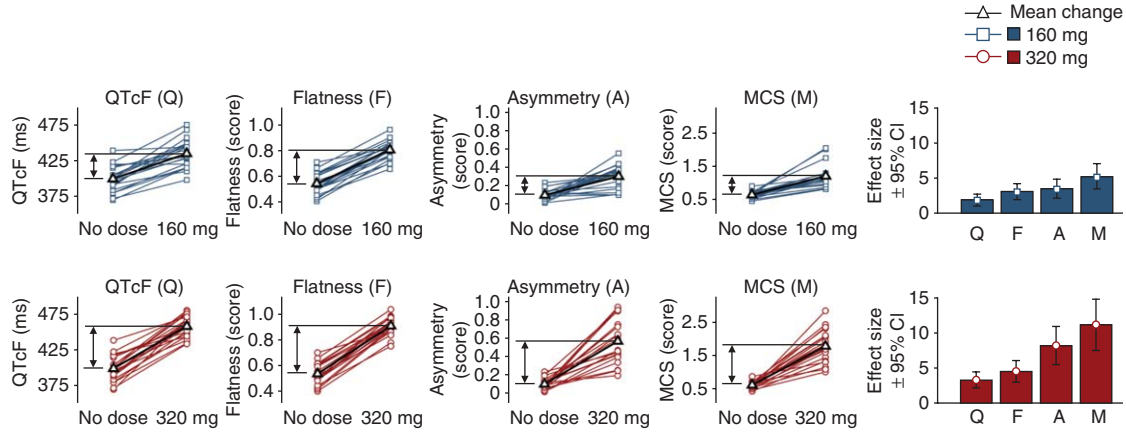

Fig. 2. Individual responses from the 21 subjects receiving sotalol at the time of maximum mean change from baseline (3.5 hours post-dose). The categorical notch measurements are not shown separately. **CI** = confidence interval; **MCS** = morphology combination score; **QTcF** = heart rate corrected QT interval.

Table II. Receiver operating characteristics (ROCs) [all recordings 0.5–3.5 h post-dose]

	QTcF		MCS		Flatness		Asymmetry		Notch	
Sotalol dose (mg)	160	320	160	320	160	320	160	320	160	320
ROC measures										
AUC ± 1 SE (%)	72 ± 3	87 ± 2	84 ± 2*	94 ± 1*	82 ± 3†	93 ± 1*	80 ± 3‡	90 ± 2	54 ± 3§	67 ± 3
Sensitivity (%)	60	73	74	88	70	83	67	84	8	27
Specificity (%)	77	93	85	88	83	90	77	80	100	100

AUC = area under the ROC curves; **MCS** = morphology combination score; **QTcF** = heart rate corrected QT interval; **SE** = standard error; * $p < 0.001$ vs AUC_{QTcF}; † $p = 0.002$ vs AUC_{QTcF}; ‡ $p = 0.015$ vs AUC_{QTcF}; § $p = 0.27$

average number of standard deviations that QTcF increased from baseline for the 320 mg dose (95% CI for the difference −0.64, 2.08), $p = 0.28$ (table III). At Δ_{max} for the 160 mg dose, T-wave morphology increased by significantly more standard deviations compared with the number of standard deviations by which QTcF increased for the 320 mg dose (95% CI for the difference 1.40, 4.69), $p < 0.001$ (table III).

T-Wave Shape

Analysis of ECG tracings revealed that T-wave morphology in subjects receiving sotalol resembled that of LQT2 patients (figure 4). Initial morphological abnormalities were primarily increased flattening of the T-wave and various degrees of asymmetry. T-wave flattening was observed within the first hour after dose for 15 of 21 subjects for the 160 mg dose and for 20 of 21 subjects for the 320 mg dose. There were 16 of 21 subjects who developed asymmetric T-waves during the first hour when the 160 mg dose was given and 18 of 21 subjects for the 320 mg dose. The appearance of distinct notches was delayed relative to the onset of T-wave flattening and the development of T-wave asymmetry. The 12-lead ECG revealed abnormal T-wave morphologies that varied between leads and even more between subjects, but were subjectively well expressed in the principal component analysis lead.

Discussion

Potential harmful effects on repolarization are of clinical and pharmaceutical interest. The electrocardiographic QT interval currently serves as the gold standard for assessment of abnormal repolarization, but other ECG indices may contribute importantly to such assessment. This study showed that a composite marker describing typical electrocardiographic LQT2 patterns could be used as a sensitive indicator of abnormal repolarization induced by the torsadogenic drug sotalol.

Identification of Abnormal T-Wave Morphology and QT Prolongation

The sotalol-induced changes in morphology of electrocardiographic T-waves were quantified with higher effect size than QTcF. The accuracy for distinguishing between baseline recordings and recordings after sotalol treatment was higher for T-wave morphology than for QTcF prolongation as well.

Taken together, our results for accuracy and effect sizes indicated that T-wave morphology identified sotalol-induced repolarization abnormalities across a broad spectrum of T-wave shape changes, from subtle to obvious. In comparison, the identification of sotalol-induced repolarization abnormalities for QTcF was less robust.

Conceivably, these differences imply that there are underlying pathological mechanisms that can be better identified by T-wave morphology than by the QT interval. Several lines of evidence support this notion. Clinically, much smaller than expected QT prolongations have been reported in patients with drug-induced TdP, whereas the onset of TdP frequently was preceded by marked changes in T-wave shapes.[35,36] A recent study of acquired bradyarrhythmias in humans demonstrated that LQT2-like morphology predicts TdP independent of the QT interval.[22]

In the rabbit model, sotalol-induced proarrhythmia can develop before any prolongation of the action potential.[37] The T-type calcium channel antagonist mibefradil, an antihypertensive that has been withdrawn from the market, caused distinct T-wave changes, often without QT prolongation, but produced TdP.[38] Moreover, a prolongation of the QT interval (i.e. by amiodarone) in the correct setting can be antiarrhythmic. Based on experimental evidence from the wedge, the antiarrhythmic effect of amiodarone was partly attributed to decreased transmural heterogeneity of repolarization, which is thought to be reflected in the TpTe interval on the ECG.[39] Clinically, however, the TpTe interval increased in patients receiving amiodarone,[40] which is not compatible with the finding of decreased transmural dispersion of repolarization. In congenital long QT syndrome, it was shown that the TpTe interval did not distinguish between symptomatic and asymptomatic patients.[41] On the other hand, convincing evidence was recently provided that the TpTe interval could be a powerful predictor for TdP in patients with acquired long QT syndrome.[42] Thus, while the experimental evidence for TpTe has been established, there are conflicting results regarding the predictive value of the TpTe interval in the clinical setting.

Most likely, prolongation of the ventricular action potential, including QT and TpTe prolongations are not the sole electrocardiographic reflections of a drug's potential to cause repolarization abnormalities. Other electrocardiographic markers might be used to more accurately identify heterogeneity of repolarization. Indeed, increased heterogeneity of myocardial repolarization could explain the occurrence of notches and the appearance of asymmetric and flat T-waves. Increased transmural, left/right ventricle and apico-basal dispersion of repolarization have been hypothesized as arrhythmic substrates in both acquired and congenital long QT syndrome,[21] and in the short QT syndrome as well.[43] Heterogeneities of repolarization are thought to be responsible for inscription of the electrocardiographic T-wave and it is thus plausible that abnormal repolarization is better identified by T-wave morphology

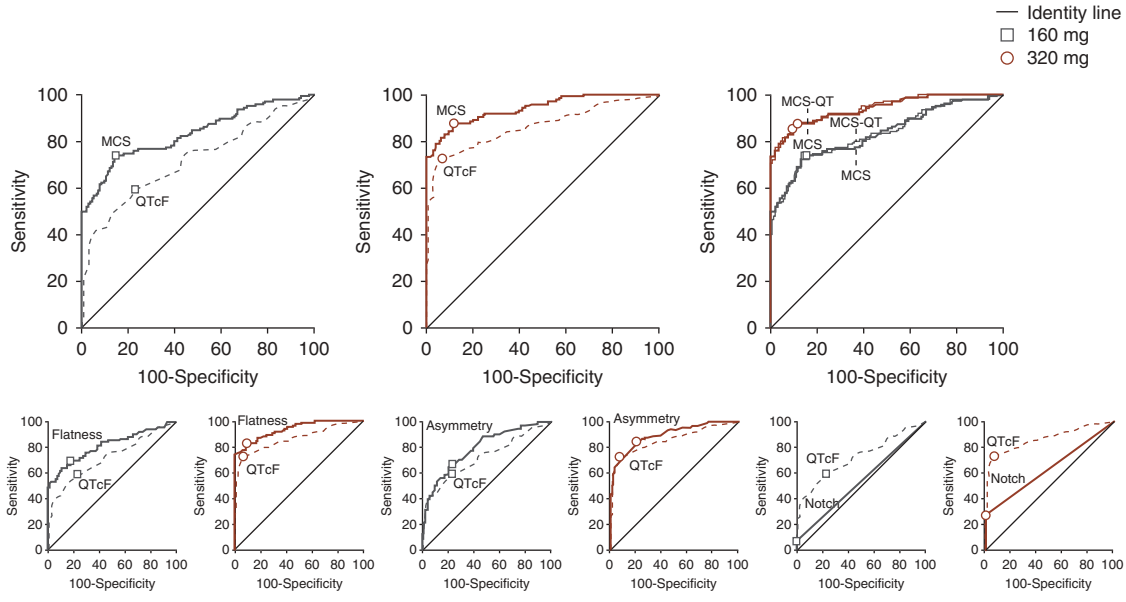

Fig. 3. Receiver operating characteristic (ROC) curves for the 21 subjects receiving sotalol. T-wave morphology was better than heart rate corrected QT interval (QTcF) at identifying sotalol-induced ECG abnormalities from the time immediately post-dose (0.5 hours) to maximum response in the mean (3.5 hours) for both the 160 and 320 mg dose. Inclusion of QTcF in the T-wave morphology measure (MCS-QT) did not improve the discrimination for morphology combination score (MCS) between baseline recordings and recordings after sotalol treatment.

than by the QT interval. Indeed, most drugs causing QT prolongation and abnormal T-waves affect the hERG channel as in LQT2. Phenotypic ECG observations in LQT2 patients would therefore be expected to be directly applicable to the identification of drug-induced repolarization effects. Invasive studies measuring Triangulation, Reverse use dependency, electrical Instability and Dispersion (TRIaD) have suggested that TRIaD may have a better predictive value for the occurrence of TdP, than the action potential prolongation (QT prolongation).[17] It is difficult to make an interpretation from the factors involved in TRIaD to the MCS measure of T-wave asymmetry, flatness and notching. It has been proposed that triangulation manifests as a broadened, more flat and notched T-wave on the ECG,[17] but to what extent such morphology characteristics are indicative of triangulation is more unclear. A thorough exploration of this relationship would require an experimental set-up with simultaneous invasive data on monophasic action potentials and ECG recordings under the influence of drugs.

Applications of T-Wave Morphology Analysis

Regulatory authorities require new drugs to be investigated in thorough ECG trials to assess potential adverse effects on cardiac repolarization. Present guidelines require that sample size be appropriate to detect a 5 ms change from baseline in the QTcF. This is a rigorous requirement considering the large intrinsic variability that is known to be associated with QT interval measurements. Measurement variability can mask the true drug-induced ECG changes and the number of subjects, which will allow a drug study to meet such stringent criteria for sensitivity, depends on the effect size. In the present study, the effect size measures for MCS and QTcF provided evidence that T-wave morphology has a lower variability at baseline and a larger difference between baseline and treatment means than QTcF. Provided that the MCS measure of T-wave morphology has general validity, these results could extend favourably to necessary sample sizes for clinical drug trials. Because the sample size (N) in a clinical trial is a function of the reciprocal of the square of the effect size at a chosen p-value and power ($C_{P,Power}$) even a modest increase in effect size can have substantial implications for the size and thus the cost of a clinical trial (equation 3).[44]

$$N \approx \frac{2}{(\text{Effect size})^2} \times C_{P,Power} \qquad \text{(Eq. 3)}$$

Importantly, sample size plays a role in ethical issues: unnecessarily large sample sizes put too many people at risk.

Our earlier work[9,15] has shown that quantified T-wave morphology can play a role in the detection of congenital long QT syndrome and we may discover other applications in the future.

Possibly, the most promising electrocardiographic marker for the identification of latent repolarization disorders is beat-beat variability of the QT interval.[25] Whether T-wave morphology

Table III. Effects of sotalol on the QT interval and T-wave morphology at the times of subject-specific peak plasma concentrations (C_{max}) and subject-specific maximum changes from baseline (Δ_{max})

Peak changes	No. of subjects	ΔQTcF (mean ± 1 SD) [ms]	ΔMCS (mean ± 1 SD)	Effect sizes	
				QTcF (95% CI)	MCS (95% CI)
Sotalol (C_{max})					
160 mg	21	28 ± 21	0.42 ± 0.33	1.84 (1.06, 2.62)	4.01 (2.58, 5.44)*
320 mg	21	52 ± 19	0.92 ± 0.44	3.40 (2.17, 4.63)	8.85 (5.89, 11.81)†
Sotalol (Δ_{max})					
160 mg	21	49 ± 13	0.84 ± 0.35	3.48 (2.25, 4.71)	7.97 (5.28 to 10.66)†
320 mg	21	75 ± 14	1.63 ± 0.52	4.92 (3.24, 6.60)	13.05 (8.70 to 17.40)†

MCS = morphology combination score; **QTcF** = heart rate corrected QT interval; **SD** = standard deviation; Δ indicates change from baseline; * $p = 0.0012$ vs effect size for QTcF; † $p < 0.001$ vs effect size for QTcF.

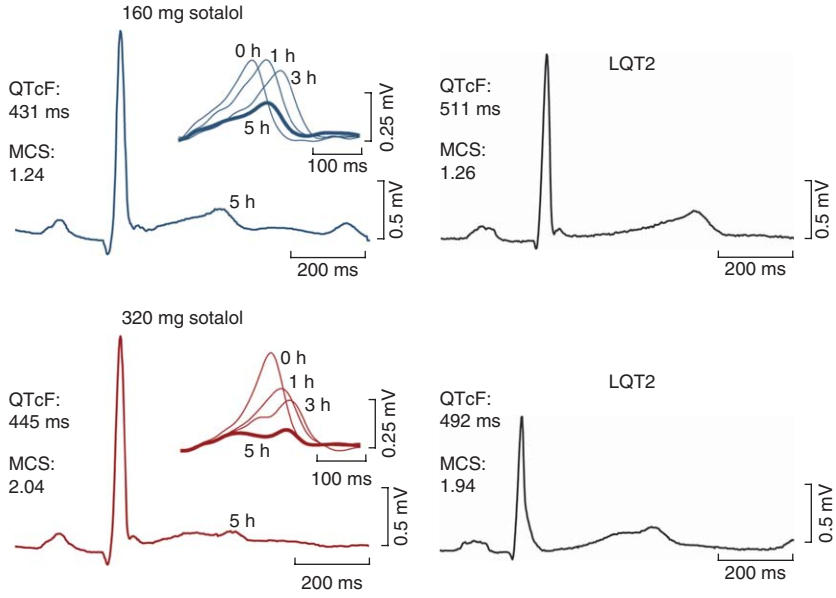

Fig. 4. ECG tracings in one subject after sotalol 160 and 320 mg (left column) compared with ECGs from patients with the type 2 form of the long QT syndrome (LQT2) [right column]. Heart rate corrected QT interval (QTcF) and T-wave morphology measures are given for the recordings 5 hours post-dose and for LQT2. Five hours post-dose, the sotalol-induced T-wave morphologies resemble T-wave morphologies in congenital LQT2 even though QTcF intervals are shorter (80 ms for 160 mg and 47 ms for 320 mg). **MCS** = morphology combination score.

might be of use for the uncovering of latent repolarization disorders and identification of patients at risk remains to be investigated. Computerized T-wave morphology analysis of ECG tracings may provide an opportunity to identify and explore complex effects on cardiac repolarization that cannot be described by the QT interval alone. An integrated assessment of QT intervals and T-wave morphology measures would possibly advance the present characterization of abnormal repolarization in congenital disease as well as for the detection of drug-induced repolarization changes. However, a standardized approach to assessing abnormal T-wave morphology on the ECG has yet to be developed and agreed on. In light of the results of the present study, we propose to conduct future studies on measurements of repolarization asymmetry, flatness and the appearance of notches, which are the typical ECG patterns in congenital LQT2. Computerized measures of T-wave morphology deserve the attention of drug safety investigators in order to reveal their possible role for the identification of drugs associated with risk.

Conclusion

A composite measure of asymmetry, flatness and the appearance of notches, which are the typical ECG patterns in congenital LQT2, were significantly altered by sotalol. The effects of sotalol on LQT2 patterns of T-wave morphology were greater than the corresponding effects on QT interval prolongation. Provided that the MCS measure of T-wave morphology has general validity for the identification of harmful drugs, this surrogate marker might therefore be used in clinical trials to support QT interval measurements when the decision to proceed with a new drug is ambiguous. Further studies are needed to validate the applicability of the MCS measure for cardiac safety evaluation.

Acknowledgements

No external sources of funding were used to support the conduct of this study. Claus Graff, Mads Andersen, Thomas Hardahl, Jørgen Kanters, Egon Toft and Johannes Struijk are authors of two filed patents describing the T-wave

morphology method. A license agreement exists between Aalborg University and GE Healthcare regarding this method. Joel Xue is an employee of GE Healthcare and owns GE Healthcare stock. Michael Christiansen and Henrik Jensen have no financial or personal conflicts of interests to report. The authors thank Pfizer Inc. for providing the data from the sotalol study.

References

1. Haverkamp W, Breithart G, Camm AJ, et al. The potential for QT prolongation and proarrhythmia by non-antiarrhythmic drugs: clinical and regulatory implications. Eur Heart J 2000; 21: 1216-30
2. Sanguinetti MC, Curran ME, Spector PS, et al. Spectrum of HERG K+-channel dysfunction in an inherited cardiac arrhythmia. Proc Natl Acad Sci USA 1996; 93: 2208-12
3. Lasser KE, Allen PD, Woolhandler SJ, et al. Timing of new black box warnings and withdrawals for prescription medications. JAMA 2002; 287: 2215-20
4. Roden DM. Drug induced prolongation of the QT interval. N Engl J Med 2004; 350: 1013-22
5. Keating MT, Sanguinetti MC. Molecular and cellular mechanisms of cardiac arrhythmias. Cell 2001; 104: 569-80
6. Sanguinetti MC, Jiang C, Curran ME, et al. A mechanistic link between an inherited and an acquired cardiac arrhythmia: HERG encodes the IKr potassium channel. Cell 1995; 81: 299-7
7. Vincent GM, Timothy KW, Leppert M, et al. The spectrum of symptoms and QT intervals in carriers of the gene for long-QT syndrome. N Engl J Med 1992; 327: 846-52
8. Zhang L, Timothy KW, Vincent GM, et al. Spectrum of ST-T wave patterns and repolarization parameters in congenital long QT syndrome: ECG findings identify genotypes. Circulation 2000; 102: 2849-55
9. Kanters JK, Fanoe S, Larsen LA, et al. T-wave morphology analysis distinguishes between KvLQT1 and HERG mutations in long QT syndrome. Heart Rhythm 2004; 1: 285-92
10. Lehmann MH, Suzuki F, Fromm BS, et al. T wave 'humps' as a potential electrocardiographic marker of the long-QT syndrome. J Am Coll Cardiol 1994; 24: 746-54
11. Malfatto G, Beria G, Sala S, et al. Quantitative analysis of T wave abnormalities and their prognostic implications in the idiopathic long-QT syndrome. J Am Coll Cardiol 1994; 23: 296-1
12. Lupoglazoff JM, Denjoy I, Berthet M, et al. Notched T waves on Holter recordings enhance detection of patients with LQT2 (*HERG*) mutations. Circulation 2001; 103: 1095-1
13. Merri M, Benhorin J, Alberti M, et al. Electrocardiographic quantitation of ventricular repolarization. Circulation 1989; 80: 1301-8
14. Benhorin J, Merri M, Alberti M, et al. Long QT syndrome: new electrocardiographic characteristics. Circulation 1990; 82: 521-7
15. Struijk JJ, Kanters JK, Andersen MP, et al. Classification of the long QT syndrome based on discriminant analysis of T-wave morphology. Med Biol Eng Comput 2006; 44: 543-9
16. Gima K, Rudy Y. Ionic current basis of electrocardiographic waveforms: a model study. Circ Res 2002; 90: 889-96
17. Shah RR, Hondeghem LM. Refining detection of drug-induced proarrhythmia: QT interval and TRIaD. Heart Rhythm 2005; 2: 758-72
18. Antzelevitch C. Heterogeneity of cellular repolarization in LQTS: the role of M cells. Eur Heart J Suppl 2001; 3 Suppl. K: K2-16
19. Couderc JP, McNitt S, Xia J, et al. Repolarization morphology in adult LQT2 carriers with borderline prolonged QTc interval. Heart Rhythm 2006; 3: 1460-6
20. Shah RR. Drug-induced QT dispersion: does it predict the risk of Torsade de pointes? J Electrocardiol 2005; 38: 10-8
21. Yan GX, Antzelevitch C. Cellular basis for the normal T wave and the electrocardiographic manifestations of the long-QT Syndrome. Circulation 1998; 98: 1928-36
22. Topilski I, Rogowski O, Rosso R, et al. The morphology of the QT interval predicts Torsade de Pointes during acquired bradyarrhythmias. J Am Coll Cardiol 2007; 49: 320-8
23. Cruz Filho FE, Maia IG, Fagundes ML, et al. Electrical behavior of T-wave polarity alternans in patients with congenital long QT syndrome. J Am Coll Cardiol 2000; 36: 167-73
24. Thomsen MB, Verduyn SC, Stengl M, et al. Increased short-term variability of repolarization predicts *d*-sotalol-induced Torsades de Pointes in dogs. Circulation 2004; 110: 2453-9
25. Hinterseer M, Thomsen MB, Beckmann B-M, et al. Beat-to-beat variability of QT intervals is increased in patients with drug-induced long-QT syndrome: a case control pilot study. Eur Heart J 2008; 29: 185-90
26. Jensen BT, Abildstrom SZ, Larroude CE, et al. QT dynamics in risk stratification after myocardial infarction. Heart Rhythm 2005; 2: 357-64
27. Couderc JP, Zareba W, Moss AJ, et al. Identification of sotalol-induced changes in repolarization with T wave area-based repolarization duration parameters. J Electrocardiol 2003; 36: 115-20
28. Guidance for industry: E14 clinical evaluation of QT/QTc interval prolongation and proarrhythmic potential for non-antiarrhythmic drugs. 2005 [online]. Available from URL: http://www.fda.gov/cber/gdlns/iche14qtc.htm [Accessed 2008 Apr 20]
29. Sarapa N, Morganroth J, Couderc JP, et al. Electrocardiographic identification of drug-induced QT prolongation: assessment by different recording methods. Ann Noninvasive Electrocardiol 2004; 9: 48-57
30. Priori SG, Mortara DW, Napolitano C, et al. Evaluation of the spatial aspects of T-wave complexity in the long-QT syndrome. Circulation 1997; 96: 3006-12
31. Andersen MP, Xue J, Graff C, et al. New descriptors of T-wave morphology are independent of heart rate. J Electrocardiol 2008; 41: 557-61
32. Andersen MP, Xue JQ, Graff C, et al. A robust method for quantification of ikr-related t-wave morphology abnormalities. Comp Cardiol 2007; 34: 341-4
33. Glass GV. Integrating findings: the meta-analysis of research. Rev Res Educ 1977; 5: 351-79
34. Hanley JA, McNeil BJ. A method of comparing the areas under receiver operating characcteristic curves derived from the same cases. Radiology 1983; 148: 839-43

35. Kay GN, Plumb VJ, Arciniegras JG, et al. Torsade de pointes: the long-short initiating sequence and other clinical features: observations in 32 patients. J Am Coll Cardiol 1983; 2: 806-17
36. Bauman JL, Bauernfeind RA, Hoff JV, et al. Torsade de pointes due to quinidine: observations in 31 patients. Am Heart J 1984; 107: 425-30
37. Hondeghem LM. Frequency dependence of class I and class III antiarrhythmic agents explaining their antiarrhythmic and proarrhythmic properties. In: Franz MR, editor. Monophasic action potentials: bridging cell and bedside. 1st ed. Armonk: Futura Publishing, 2000: 381-94
38. Benardeau A, Weissenburger J, Hondeghem L, et al. Effects of the T-type Ca^{++} channel blocker mibefradil on repolarization of guinea pig, rabbit, dog, monkey, and human cardiac tissue. J Phamacol Exp Ther 2000; 292: 561-75
39. Sicouri S, Moro S, Litovsky S, et al. Chronic amiodarone reduces transmural dispersion of repolarization in the canine heart. J Cardiovasc Electrophysiol 1997; 8: 1269-79
40. Smetena P, Pueyo E, Hnatkova K, et al. Effect of amiodarone on the descending limb of the T wave. Am J Cardiol 2003; 92: 742-6
41. Kanters JK, Haarmark C, Vedel-Larsen E, et al. TpeakTend in long QT syndrome. J Electrocardiol 2008; 41: 603-8
42. Yamaguchi M, Shimizu M, Ino H, et al. T wave peak-to-end interval and QT dispersion in acquired long QT syndrome: a new index for arrhythmogenicity. Clin Sci 2003; 105: 671-6
43. Extramiana F, Antzelevitch C. Amplified transmural dispersion of repolarization as the basis for arrhythmogenesis in a canine ventricular-wedge model of the short-QT syndrome. Circulation 2004; 110: 3661-6
44. Whitley E, Ball J. Statistics review 4: sample size calculations. Crit Care 2002; 6: 335-41

Correspondence: *Claus Graff*, SMI, Department of Health Science and Technology, Aalborg University, Fredrik Bajers Vej 7 E1-209, 9220 Aalborg, Denmark.
E-mail: cgraff@hst.aau.dk